# Second harmonic generation via total internal reflection quasi-phase-matching in a hexagonal nonlinear optical microresonator

Tleyane J. Sono*[a], Christos Riziotis[b], Sakellaris Mailis[a], Robert W. Eason[a]
*tjs@orc.soton.ac.uk

a. Optoelectronics Research Centre, University of Southampton, Highfield, Southampton, SO17 1BJ, U.K.
b. Department of Telecommunications Science and Technology, University of Peloponnese, 22100, Tripoli, Greece

**Abstract:** *We propose the enhancement of the second harmonic generation process in an optical hexagonal microcavity, consisting of a nonlinear material, via total internal reflection quasi-phase-matching technique. We present preliminary numerical simulation results showing resonance operation in a suitably designed hexagonally shaped optical microresonator, which demonstrates the operating feasibility of the proposed scheme. The SHG efficiency was calculated using lithium niobate as the nonlinear material. High optical quality hexagonal superstructures can be manufactured routinely by chemical etching of inverted ferroelectric domains in this material.*

## Introduction

Quasi-phase-matching (QPM) is a technique commonly used to enhance the efficiency of nonlinear interactions, such as second harmonic generation, (SHG), in cases where full phase-matching cannot be applied. One example of QPM SHG is by periodic poling in lithium niobate or KTP where the sign of the relevant nonlinear *d* coefiecient is inverted every coherence length ($l_c = \pi / \Delta k$) to compensate for the phase error between the fundamental wave (FW) and the second harmonic (SH) wave caused by the dispersion of the nonlinear medium. Another way to achieve quasi-phase-matching is by utilising the relative Fresnel phase shift ($\Delta\Phi_F$) between the FW and SH, induced upon total internal reflection (TIR) of the two waves at the medium-air interface to compensate for the dispersion phase mismatch ($\Delta kl$) as reported in ref[1]. The phase shift $\Delta\Phi_F$ in TIR-QPM, depends on: (1) the reflection angle, which always exceeds the critical angle, (2) the refractive indices of the propagation and surrounding media and (3) on the input/output polarization of the propagating waves [2]. The effective nonlinear *d* coefficient ($d_{eff}$) can also change sign after reflection depending on the selection of the input/output polarization which will result in an extra phase shift ($\xi\pi$) with $\xi$ being 1 or 0 depending on the inversion of $d_{eff}$. Above the critical angle, the combination of $\Delta\Phi_F$ and $\xi\pi$ can take any value between 0 and $2\pi$ allowing for more flexibility for the propagation length between adjacent reflections as compared to the periodic poling case where the $2l_c$ period constraint is strict. TIR-QPM has been demonstrated and analysed in planar geometries for semiconductor materials.[2, 3] In this contribution we propose TIR-QPM in a hexagonal nonlinear optical microcavity where the FW is resonantly enhanced which subsequently increases the efficiency of the non-linear process while maintaining the small device size.

Micro-cavities have attracted much attention due to their wide range of functionalities and their small size which enables dense integration. Hexagonal microcavities in particular exhibit advantageous long input/output-coupling lengths, hence the coupling gap is not limited to the sub-micron bottleneck imposed on other geometries e.g. micro ring resonators. Most of the work on resonators demonstrated to date is focussed however on filtering applications such as add-drop filters. However this paper considers nonlinear phenomena with the principal aim to demonstrate the use of the hexagonal microcavity for an efficient SHG process by utilising the power build-up in an optical resonator. The choice of the hexagonal geometry is due to the fact that hexagonal optical cavities of superior optical quality can be fabricated by differential etching of inverted ferroelectric domains in lithium niobate.[4] Additionally, lithium niobate possesses a large $d_{33}$ coefficient and hence, along with the fabrication argument constitutes a good candidate for the demonstration of TIR-QPM in this microcavity geometry.

Ma *et. al.*[5, 6] have studied the incident angle dependence of the optical power build-up in a hexagonal cavity showing an increase of number of cavity round trips resulting in sharp resonance for a reflection angle of 60°. Only at this angle can the length between subsequent reflections be constant and support long lived resonances with high Q. This restriction is also critical for QPM operation inside the cavity, as in the studied technique here. As shown in fig.1 the FW is being launched within the cavity (at the "source" position) in order to maintain the 60° reflection angle. We followed this launching approach instead of the side evanescent wave coupling in order to focus this initial work on the operational principle rather than on technical issues such as the design of side coupling sections. At this reflection angle, we avoid open-loop trajectories which although they also lead to cavity resonance

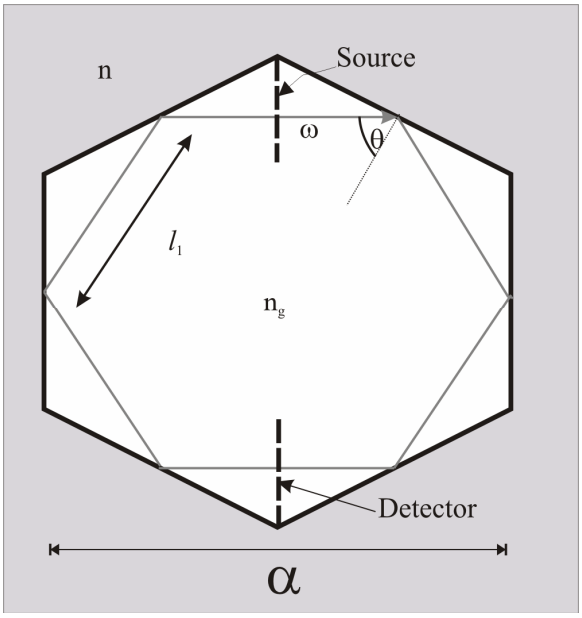


**Fig. 1**: Regular hexagonal optical cavity showing the optical path of the fundamental wave ω. α is the distance between opposite walls and $l_1$ is the propagation length between sequential reflections.

modes (provided they are waterfront-matched after each cavity round-trip) , they however have a short cavity life-time.[5, 6] A reflection angle of 60° also guarantees that the length ($l_1$) between subsequent TIRs in the regular hexagonal cavity is equal, which simplifies the expression for phase compensation.

The first step of the analysis will be to determine by a simplified but effective analytical model the optimal cavity size which supports both a resonance for the FW and provides TIR-QPM for second harmonic generation.

**Theoretical Approach**

The condition for TIR-QPM is given by the following expression[7]:

$$\phi = \Delta k l_1 + \Delta\Phi_F + \xi\pi = 0 \bmod 2\pi \text{ . Eq. 1}$$

Simultaneous resonance of the FW and SH wave is possible provided that the following conditions are satisfied[7]:

$$k^{\omega} l_1 + \Phi^{\omega} = 0 \bmod \pi \quad \text{Eq. 2}$$

$$k^{2\omega} l_1 + \Phi^{2\omega} = 0 \bmod \pi \quad \text{Eq. 3}$$

$\Phi^{\omega}$ ($\Phi^{2\omega}$) and $k^{\omega}$ $l_1$ ($k^{2\omega}$ $l_1$) are the Fresnel and dispersion phase shift of FW (SH wave) on reflection. Upon propagation of FW along $l_1$, SH signal is generated, with optimum efficiency provided that the TIR-QPM condition is satisfied. To satisfy both the resonance of FW and SH waves and TIR-QPM condition,

**Table 1:** Results of the cavity dimension at different values of $\lambda_{\omega}$

| $\lambda_{\omega}$/μm | α/μm | $l_c$/ μm |
|---|---|---|
| 0.900 | 3.369 | 1.956 |
| 1.000 | 5.133 | 2.788 |
| 1.064 | 5.973 | 3.401 |
| 1.200 | 8.978 | 4.899 |
| 1.550 | 17.47 | 9.512 |

a suitable cavity size is determined by identifying an appropriate $l_1$ that simultuneously satisfies all eqs (1-3) for a given wavelength (λ).

The intensity of the generated SH ($I_{2\omega}$), (assuming no depletion of the FW), can be written as[3]

$$I_{2\omega} = \frac{8\pi^2 d_{eff}^2}{n_{\omega}^2 n_{2\omega} \lambda_{\omega}^2 \varepsilon_0 c} I_{\omega}^2 l_1^2 \left[\frac{\sin(\Delta k l_1/2)}{\Delta k l_1/2}\right]^2 \times \left[\frac{\sin(N\phi/2)}{\sin(\phi/2)}\right]^2 \text{ . Eq. 4}$$

where N is the number of TIR reflections within the cavity, $I_{\omega}$ is the FW intensity and $\lambda_{\omega}$ is the wavelength of the FW. Here, unlike the case of resonant TIR-QPM, $l_1$ does not have to be an exact odd multiple of the coherence length.[2] The value of $l_1$ is determined by the balance between the dispersion and the relative Fresnel phase shift.
The results of the numerical calculations for the determination of a suitable cavity size and the cavity characteristics showing the resonance of FW for lithium niobate are shown below. Also we show numerical results for the SHG efficiency.

**Results**

A suitable cavity size was determined by combining the phase matching condition (equation (1)), and wave propagation conditions for FW and SH wave (equations (2-3)) resulting in the following equation[7].

$$\cos(0.5(\Delta k l_1 + \Delta\Phi_f + \xi\pi)) \times \cos(k^{\omega} l_1 + \Phi^{\omega}) \times \cos(k^{2\omega} l_1 + \Phi^{2\omega}) = \pm 1 \quad \text{Eq. 5}$$

In the cavity geometry as shown in figure 1 the z axis of the $LiNbO_3$ crystal is normal to the page and each side of the cavity is along a y-axis of the

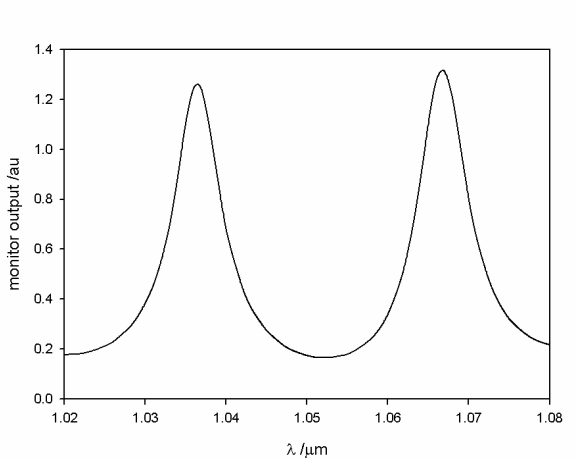


**Fig. 2:** FSR for FW in a z-cut $LiNbO_3$ regular hexagonal micro-cavity when $\alpha = 5.973$ μm.

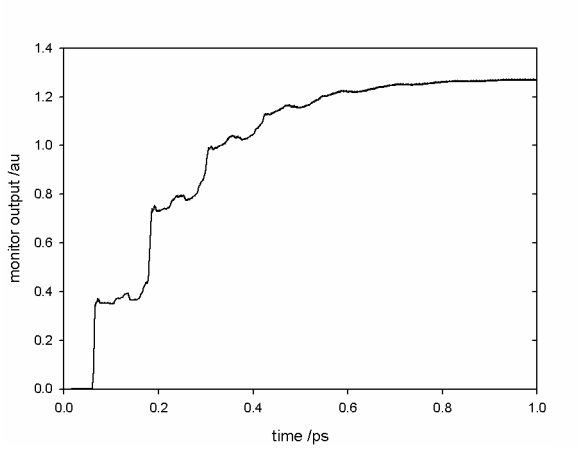


**Fig. 3:** Cavity build-up for FW in a z-cut $LiNbO_3$ regular hexagonal micro-cavity for $\lambda_\omega = 1.064$ μm.

crystal. In this particular z-cut $LiNbO_3$ cavity geometry, $d_{eff} = d_{33}$ and does not change sign when both FW and SH wave have a polarization parallel to the plane of incidence. Here we consider the first order TIR-QPM as corresponding to the smallest cavity size which satisfies eq (5). Solving eq (5) using the dispersion and Fresnel parameter for a z-cut lithium niobate crystal at a given $\lambda_\omega$ and an incidence angle $\theta = 60^o$ determines the values of $l_1$ and subsequently the cavity size ($\alpha = 2l_1$) that simultaneously satisfies the FW and SH wave propagation and TIR-QPM conditions. Table 1 contains the cavity dimensions and the coherence lengths determined for the first-order TIR-QPM for a cavity at different values of $\lambda_\omega$.

A 2-D FDTD simulation tool was employed to carry out the simulation work. Steady-state solutions were obtained for the cavity free spectral range (FSR) and optical power build-up for the FW and SH. The following parameters were employed in this calculation: A c.w. beam at $\lambda_\omega$ (TM polarized, $n_g = n_e(\lambda_\omega)$ and n = 1) was launched from the "source" position in a microcavity and detected by an overlap monitor as shown in fig. 1. Fig. 2 shows the FSR for FW in the micro-cavity with $\alpha = 5.973$μm which corresponds to a solution of eq (5) optimised for TIR-QPM and propagation of both FW and SH wave at $\lambda_\omega = 1.064$ μm. This numerical result was achieved by varying the exciting wavelength for this cavity. The values in fig. 2 are measured after 1ps, (which is long enough to allow steady state to be reached. The FSR is ~ 30 nm which is in good agreement with the theoretical estimate $FSR \approx \lambda^2/3n_g\alpha$ for $\theta = 60^o$.[5] Fig. 3 shows the optical power build-up in the cavity for $\lambda_\omega = 1.064$ μm which reaches a steady state after approximately five round trips (0.8 ps) after which the signal loss balances the input source. The steady state power of the FW can be used to calculate the power of the SH wave. Each cavity round-trip equals six reflections. The FW power in the cavity is maximum after five round-trips which implies N= 30. This N value was used in equation (4) to estimate SHG yield and conversion efficiency. Fig.4 shows a plot of the normalized SH signal growth per round-trip in the cavity. Each curve in the plot of fig. 4 shows the power of the SHG as a function of the reflection angle after a specific round trip. The SH signal growth is about 80% of the maximum obtainable SHG efficiency for $\theta = 60^o$ after five round trips.

**Discussion**

Microresonators form a very favourable solution for high density integrated optics suitable for a variety of applications, from sensing, to high channel count optical filters for DWDM systems. The integration of additional nonlinear functionalities, such as second harmonic generation will strengthen their role and make more compatible the use of microresonators in integrated optics circuitry. The proposed scheme for SHG via TIR-QPM in a hexagonal microcavity can improve the efficiency and also the compactness of SHG devices compared to traditional linear-type based devices. Based on a simple theoretical model the optimal cavity size could be easily determined. Furthermore numerical simulation results based on Beam Propagation analysis confirmed the solutions obtained by demonstrating resonant operation of the microcavity first in the FW and also in the SH wave produced by TIR-QPM. These results suggest the feasibility of this proposed scheme that could also be extended to higher order polygons.

Although it is evident from the simulation results that the hexagonal optical cavity considered here is a lossy optical structure, this is due to the sharp corners of the cavity. This is a common problem in polygonal resonators and can degrade also the performance of passive devices such as add-drop filters. Lately the use of smoothed round cornered polygonal microresonators has shown the improvement in the Q factor and finesse in such devices[8]. This rounding

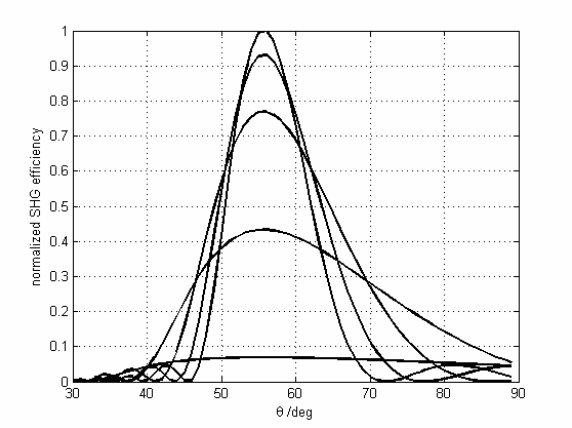


**Fig. 2**: Growth of the SH wave per round trip in the cavity as a function of the reflection angle. The curve with the highest peak value coresponds to the 5th successive roundtrip.

improved in turn, drastically the actual filtering characteristics of those devices.

However it should be stressed here that the sole purpose of this work is to introduce and demonstrate the concept of SHG via TIR-QPM inside a resonant cavity. Further work is currently in progress in order to consider improved and more realistic implementation of this scheme with hexagonal cavities, or even circular cavities, with the expectation of improving the SHG efficiency. We will further discuss the optimization of such a scheme based on these preliminary results.

## Conclusions

We have numerically demonstrated the enhancement of SHG efficiency via TIR-QPM by utilising the resonance of the fundamental beam within a hexagonal micro-cavity with suitable dimensions. Lithium niobate can serve as a useful platform to demonstrate and implement effectively the proposed process because of its high non-linearity and its preferred hexagonal shaped which results during chemical etching of the inverted ferroelectric domains.

**Acknowledgment**
The authors would like to thank the commonwealth Scholarship for T. J. S, the University of Southampton alleviation fund, the EPSRC Portfolio Partnership in Photonics EP/C515668/1 and the EU STREP 3D-DEMO for financial support.

**References**

1 J. A. Armstrong, N. Bloembergen, and J. D. P. S. Pershan, Phys. Rev. **127**, 1918 (1962).
2 R. Haidar, N. Forget, P. Kupecek, and E. Rosencher, J. Opt. Soc. Am. B **21**, 1522 (2004).
3 H. Komine, W. H. long, J. W. Tully, and E. A. Stappaerts, Opt. Lett. **23**, 661 (1998).
4 C. L. Sones, S. Mailis, W. S. Brocklesby, R. W. Eason, and J. R. Owen, J. Mater. Chem. **12**, 295 (2002).
5 N. Ma, F. K. L. Tung, S. F. Lui, and A. W. Poon, in *Proc. SPIE*, Photonics West Conference, San Jose, California, 2003), Vol. 4986.
6 N. Ma, in *Dept. Elec. and Electron. Eng.* (The Hong Kong Univ. of Science and Tech., 2004), Vol. MPhil.
7 R. Haidar, Appl. Phys. Lett. **88**, 211102 (2006).
8 C. Li and A. W. Poon, Opt. Lett. **30**, 546 (2005).